Automated Infusion Repair on Rotor Blades – Improving Quality Standards

Gefördert durch:

Bundesministerium für Wirtschaft und Technologie

aufgrund eines Beschlusses des Deutschen Bundestages

Dipl.-Ing. Markus Zellhuber
Airbus Helicopters Deutschland GmbH
Industriestr. 4
86609 Donauwörth
GERMANY

Markus.Zellhuber@airbus.com

Co-Author:

Dipl.-Ing. Hannes Schmid
Airbus Helicopters Deutschland GmbH
Industriestr. 4
86609 Donauwörth
GERMANY

Hannes.Schmid@airbus.com

ABSTRACT

Aerospace components in aviation industry have been repaired by manual splicing and subsequent wet laminating for decades. These methods are tested in practice, but are still not approved for structural repairs (where the component has no limit-load capacity without repair), although the demand for such kind of repairs grows daily. This is mainly due to the lack of confidence in process reliability during bonding, due to the many manual process steps. For this reason, Airbus Helicopters has been working on the improvement and step-by-step automation of these processes, in the field of rotor blade repair for several years, in order to meet the high certification requirements. This document provides an overview of the applications in the field of rotor blades, the current process chain of bonded blade skin repairs, approaches to the automation of the entire process chain and their approval, as well as an outlook in the future of bonded primary structures.

1.0 INTRODUCTION

With the increasing number of helicopter main rotor blades flying, the number of repairs increases as well. Since repair work is generally cost efficient for high-value components such as rotor blades, Airbus Helicopters has developed a repair instruction for standard damages due to fatigue, erosion and foreign objects. This repair instruction defines both, the permissible repair size limits and areas as well as the associated bonding process. At present, the process chain for rotor blade repairs is as follows:

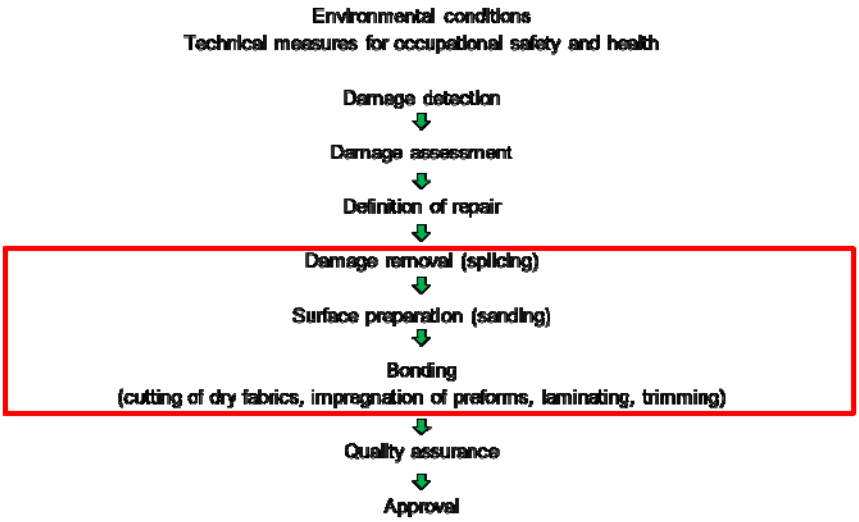

Figure 1-1: Process chain for rotor blade repairs.

However, only the process steps of splicing, surface preparation, laminating and curing, which are marked in red in Figure 1-1, are important for the improvement of the bonding, which is why they should be further considered in detail. On the basis of the results of the research projects Rapid Repair, CAIRE (Composite Adaptable Inspection and Repairs) and FACTOR (Future Advanced Composite Bonding and bonded Repair), the process chain illustrated in Figure 1-2 shall gradually replace the current repair process.

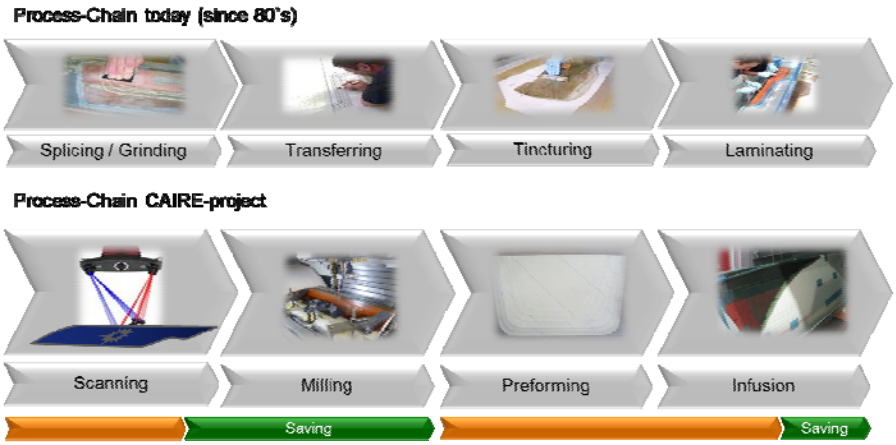

Figure 1-2: Comparison of repair process-chain.

In order to exclude human influences as far as possible during the splicing of the repair area, the new process is based on an automated milling. The previous manual impregnation and laminating of the repair plies should be replaced by a dry preform, impregnated via an infusion process. Both methods offer the possibility to generate reproducible results, within certain tolerances, by definition of the process parameters.

2.0 DEVELOPMENT OF NEW PROCESSES

Extensive attempts to determine suitable process parameters were necessary for the successful implementation of the new processes. Moreover, not only the feasibility but also the actual improvement of the bond should be demonstrated. The following chapter therefore deals with the investigation and definition of the process parameters for all steps in detail.

2.1 3D-Scan of repair area

The basis for the generation of the milling paths and the subsequent splicing is a scan of the component, more precisely the area to be repaired of this component. Because all other steps are based on this digital scan, the accuracy of scanning is critical. The aim is to achieve a measurement uncertainty of max. 0.05mm. Modern scanning systems such as the "GOM Atos III triple scan" have a very high accuracy, which is however influenced by the reflection properties of the surfaces. Especially in the case of GFRP components, but also in the case of CFRP components, this is a challenge because of the translucent resin surfaces. The scanning experiments in the project showed that the accuracies on grinded surfaces can be achieved, but the accuracies on untreated surfaces are highly dependent on the incidence angle of the scanner light. Figure 2-1 shows an overview of the interrelationships and experiments at Airbus Group Innovations on untreated resin surfaces:

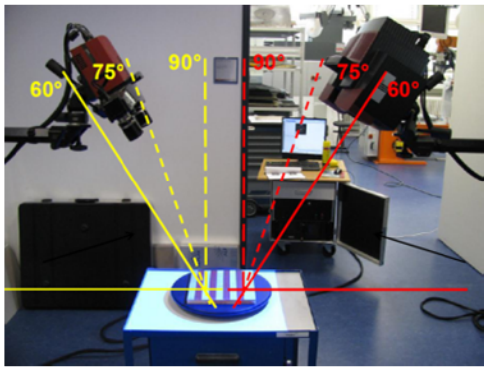

Scanning Angle	Average Deviation
60°	0,07mm
75°	0,04mm
90°	0,015mm

Figure 2-1: Scanning accuracy depending on scanning angle. (Source: Airbus Group Innovations)

2.2 Repair splicing by milling

The generation of milling paths on the basis of the scanned surface is necessary for the subsequent milling of the splice. For this purpose, a special software was developed within the projects RAPID REPAIR and CAIRE in collaboration with iSAM AG. The software is able to calculate the corresponding milling paths by defining an arbitrary inner contour and outer contour or by defining an associated splicing ratio. It does not

matter which scanning system (point laser, line laser, fringe pattern projection, etc.) is used or to which machine (robot, milling portal, etc.) data are sent. This is particularly important as the system is to be used not only for dismountable components such as rotor blades, but also directly on the aircraft (done by a mobile robot). A particularly complex shape of a repair-splicing of a rotor blade can be seen in Figure 2-2 (screenshot out of the software).

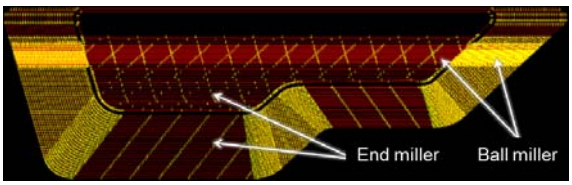

Figure 2-2: Milling tracks for blade skin repair. (Source: Isam AG)

In order to make the milling process as efficient as possible and suitable for complex structures with small radii, different milling tools have to be used. In the case of a skin repair on the rotor blade, both end miller cutters with corner radius (torus cutter) as well as ball millers are used. The result of such a milled repair splicing is shown in Figure 2-3.

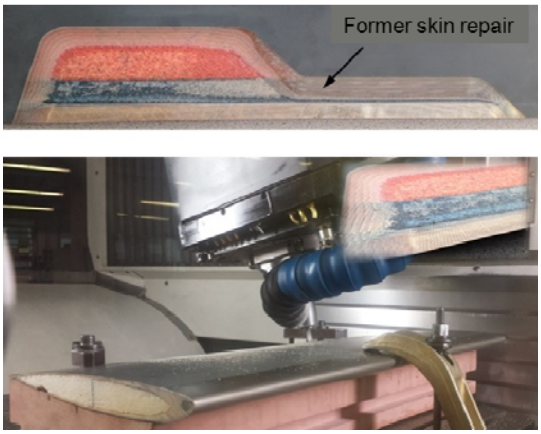

Figure 2-3: Milling of blade skin repair.

The accuracies achieved in this way depend on the milling machine (robot / portal) used and are comparable to manually spliced repairs. The homogeneity of such splices can be significantly increased even with less precise milling machines (see Figure 2-4).

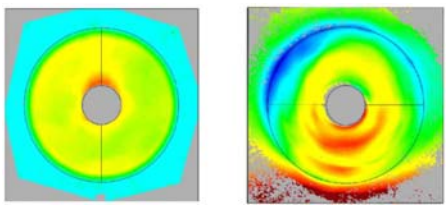

Figure 2-4: Comparison: Splicing done by robot vs. manually grinded.

2.3 Investigation of milling parameters

In order to demonstrate the same repair strength for automatically spliced repairs compared to the certified manually grinded ones, a coupon test program was started. Essentially, G1C and spliced tensile specimens were used, whereby the latter is to be discussed separately here. For the coupon program, "extreme" milling parameters (very low / high tool offset, very low / high feed rate, etc.) were selected to generate a wide parameter field for later use. Furthermore, it should be investigated whether the bonding strengths achieved can be predicted by measuring special surface properties before bonding. For this purpose, surface characterizations were carried out prior to bonding using different measuring methods. In addition light microscope images were created.

2.3.1 Investigation of surface properties

First of all, it was discovered that the resulting surfaces differed widely visually and haptically. This was already visible without enlargement by the light microscope and can be seen in Figure 2-5 as well.

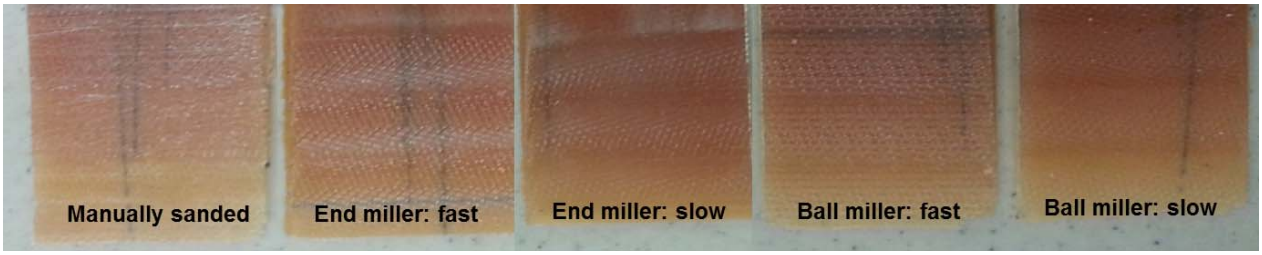

Figure 2-5: Milled surfaces without magnification.

On the basis of light microscopy images in various magnification levels, characteristics such as fiber tears, milling marks and impurities of the milled repair surfaces could be recognized. These microscope images served to provide an optical impression of the surfaces. All light microscopy images were taken by the consortium partner Airbus Defense & Space in Manching.

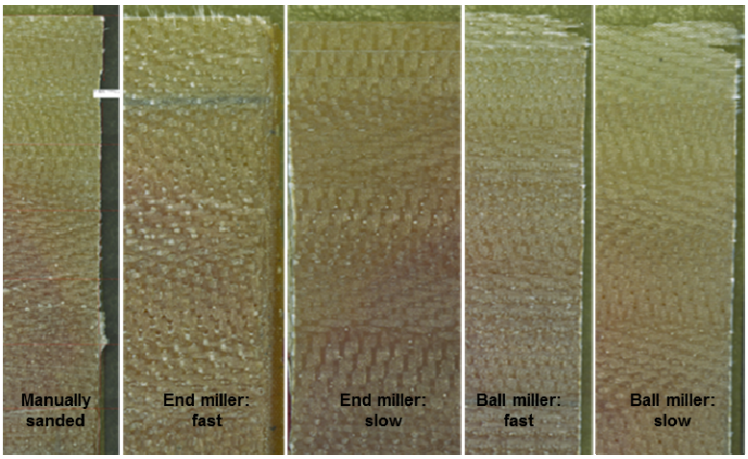

Figure 2-6: Milled surfaces at 20-times magnification.

Figure 2-6 shows the milled surfaces at 20-times magnification. The inhomogeneous surface of the hand-grinded sample compared to the machined samples was already clearly visible on these images. Tool marks (in the case of surfaces of the ball milling cutter, for example) could also be identified. Finally, images at a

1000-times magnification were taken. These are shown in Figure 2-7. In contrast to the previously shown pictures, there was no difference between manual and automated production parameters visible. Even the fiber tears visible on the surface immediately after milling (in case of the fast parameter sets) seemed to have been removed by cleaning with an acetone impregnated lintfree cloth. Due to the high magnification, regions with differently sized resin nests ("milky" areas of the image) were visible. However, no direct link to the milling parameters could be established.

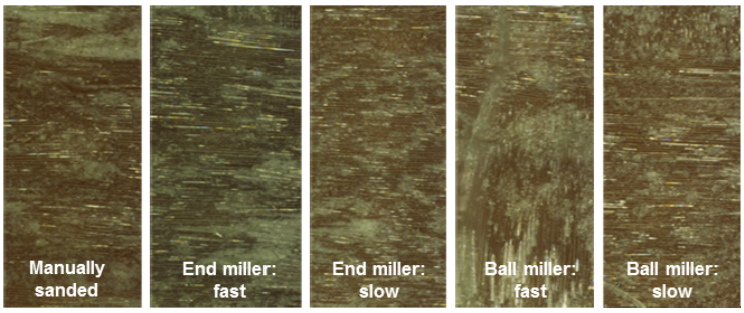

Figure 2-7: Milled surfaces at 1000-times magnification.

The surfaces were then optically measured by means of the focus variance microscopy. The process described below as an Alicona measurement (Alicona = Name of manufacturer) has the great advantage (depending on the resolution) of giving surface roughness values, as well as a percentage increase in the effective surface due to roughness. These values were thought to be potentially significant values for the strength of an adhesive bond. All Alicona measurements were also carried out by the consortium partner Airbus Defense & Space. Since very large amounts of data are generated during an Alicona measurement, the measuring procedure is very time-consuming and the entire sample could not be measured. Instead of the entire sample, approximately 6 mm long and approximately 2 mm wide strips, transversely to the milling direction were measured. The fact that the Alicona measurements of the surfaces with a splicing ratio of 1:60 are transferable on surfaces with a splicing ratio of 1:10 was demonstrated by means of a verification measurement. The results of all measurements are shown in Figure 2-8.

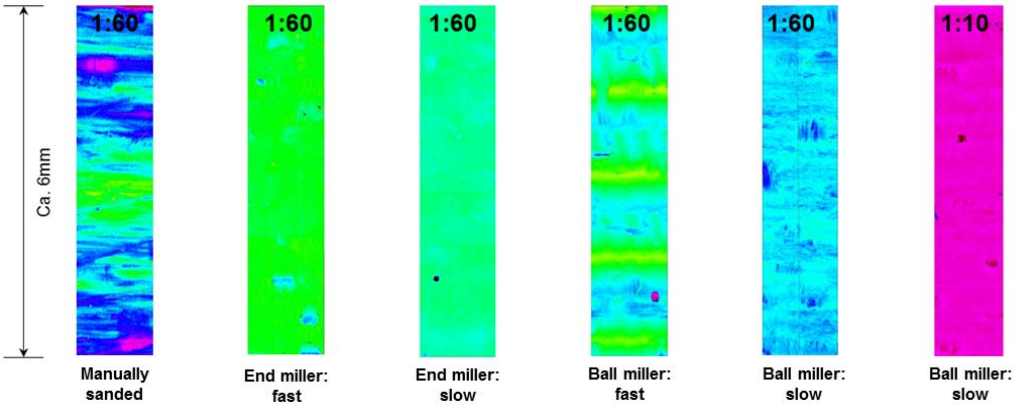

Figure 2-8: Alicona measurements.

In the Alicona measurements, it became clear that the fast machining parameters with the ball miller achieved the highest roughness values. In a "medium" roughness range of the series the fast milling parameters with the end miller and the manually grinded surfaces can be found. The slow milling parameters provided the "smoothest" surfaces of the sample program with both milling tools. Therefore, the surface

magnifications for these parameter are relatively small. The tactile roughness measurements of the samples were carried out in the form of a classical sampling pattern. In order to obtain an preferably representative image of the surface, three measurements were taken in and across the milling direction. This scheme is shown in Figure 2-9.

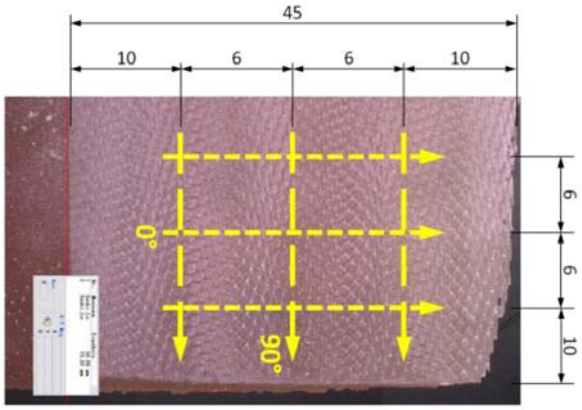

Figure 2-9: Measurement scheme for tactile roughness values.

The mean value of the individual measurements was used to evaluate the roughness measurement. The overall picture of the measurements was able to confirm the tendency from the Alicona measurements, even when the maximum values did not fit exactly in the absolute dimension. In addition to the pure roughness values, the profiles of the individual surfaces were also characterized. In this way, clear "patterns" of the milling tools could be recognized on the surface. As a particularly clear example, Figure 2-10 shows the processing parameters of the fast ball milling cutter.

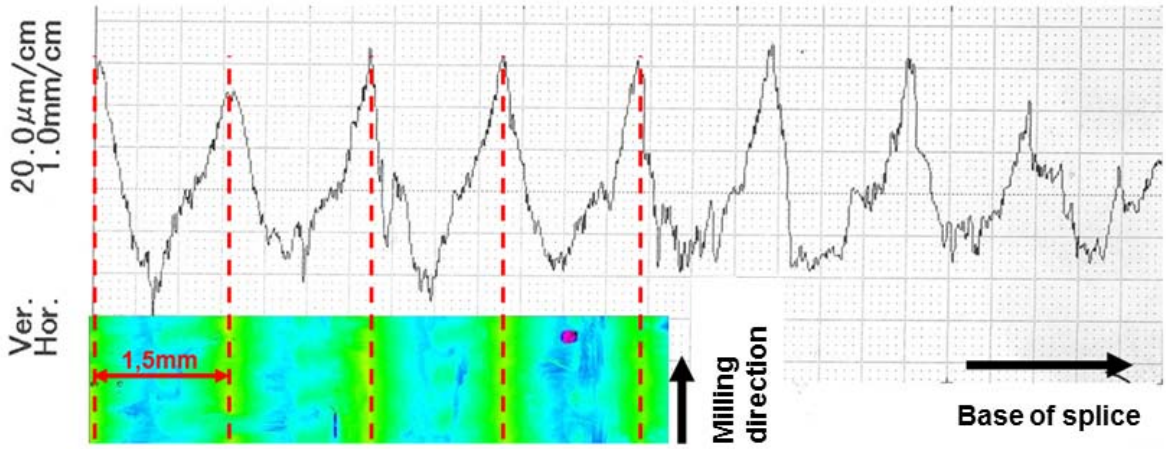

Figure 2-10: Alicona measurement compared to tactile roughness measurement.

The characteristic patterns and associated mean values of the roughness measurements are plotted in Figure 2-11.

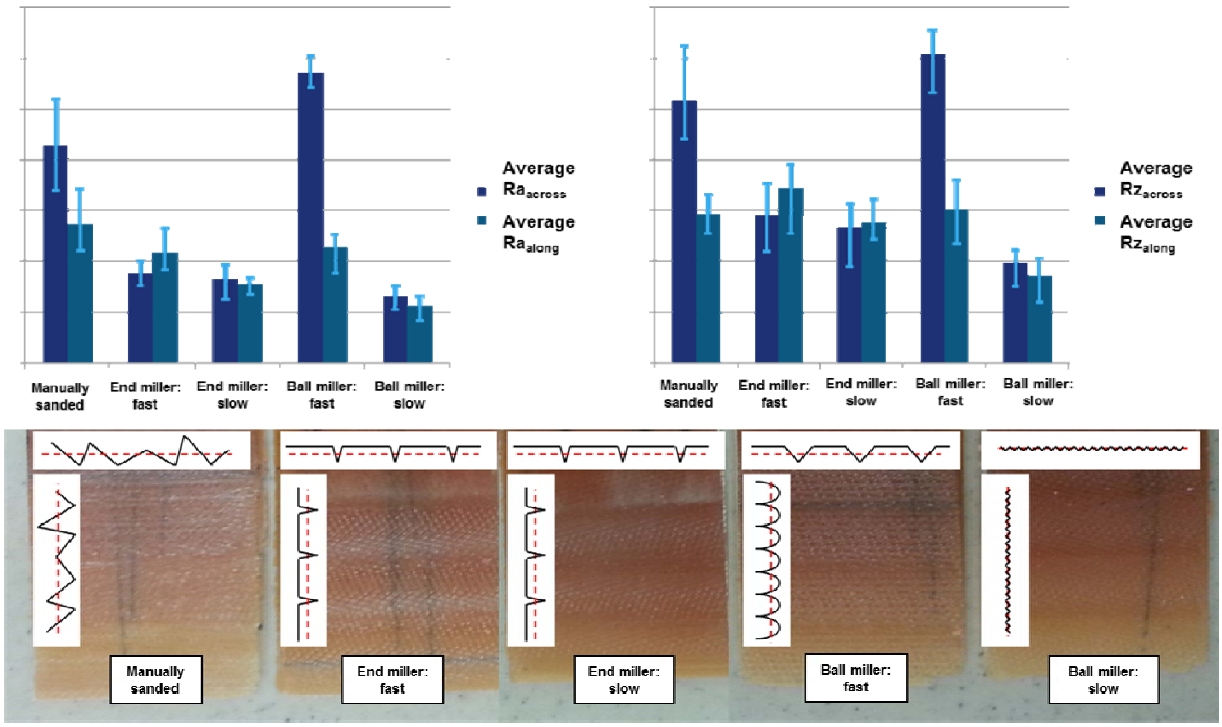

Figure 2-11: Results of tactile roughness measurements.

2.3.2 Mechanical tests

In order to detect differences in the adhesive strength caused by different morphological characteristics of the bonding surface of the splice (and thus the used milling parameters) with a repaired tensile specimen, it is necessary to cause adhesive failure of the bonding. In order to achieve this failure, the tensile specimens were produced with a splicing ratio of 1:10. With this low splicing ratio, the safety margin of the bonded joint is in the range of 1 and an adhesive failure of the bond can be expected. The exact shape of the coupons is shown in the drawing in Figure 2-12. For the determination of the repair strength only, tensile specimens made with the splicing ratio of 1:60 were used.

Five samples with a splicing ratio of 1:10 could be tested for each milling parameter at the “Institut für Flugzeugbau” of the University of Stuttgart. The specimens were tested without pre-load and were instrumented on both sides with strain gauges in and diagonally to the pull direction in order to take into account the different strengths / elongations of the repair and basis material. The evaluation of the tensile tests with the splicing ratio of 1:10 was focused on the tensile strengths and the shear strengths of the repair bond. The bonding surface for the calculation of the shear strength was measured on the sample directly before the tensile test. If the sample did not fail within the bond, the shear strength value had to be regarded as a minimum value. In Figure 2-12 the type of failure for each series of tensile specimens is shown exemplary.

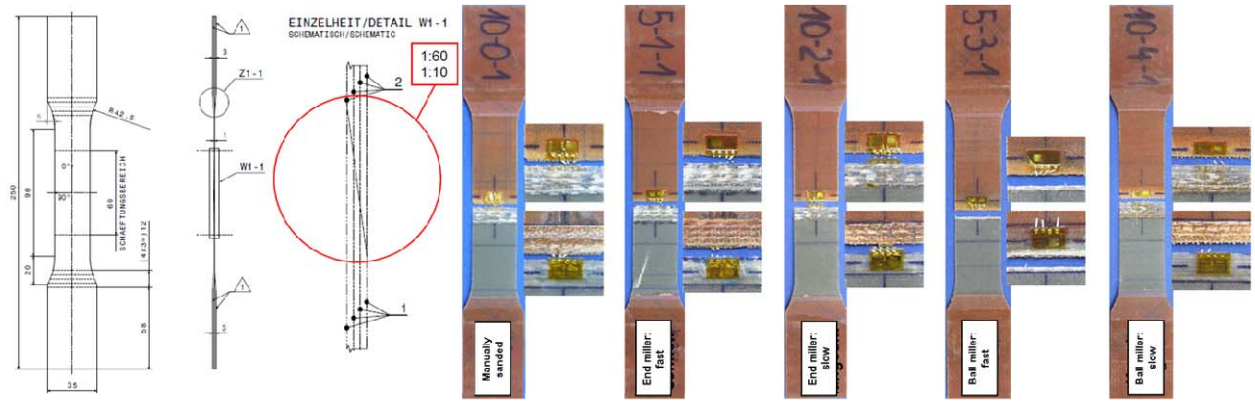

Figure 2-12: Fracture pattern of spliced tensile specimen 1:10.

At first it was noticeable that in case of the "end miller slow" parameter set, only one sample failed in the bonding area and, in case of the parameter set "ball miller fast" even no single specimen showed a correct failure. In this case, all samples failed in the area of the repair laminate. For the evaluation, the mean values of the strain gauges on the front and rear side were used and it could be clearly stated that the machined specimens show a significantly lower scatter in the tensile strength values. This effect again suggests the higher process reliability of the milled samples. Furthermore it became clear that the tensile strength values of all parameter sets do not show any extreme differences in the absolute values (see Figure 2-13).

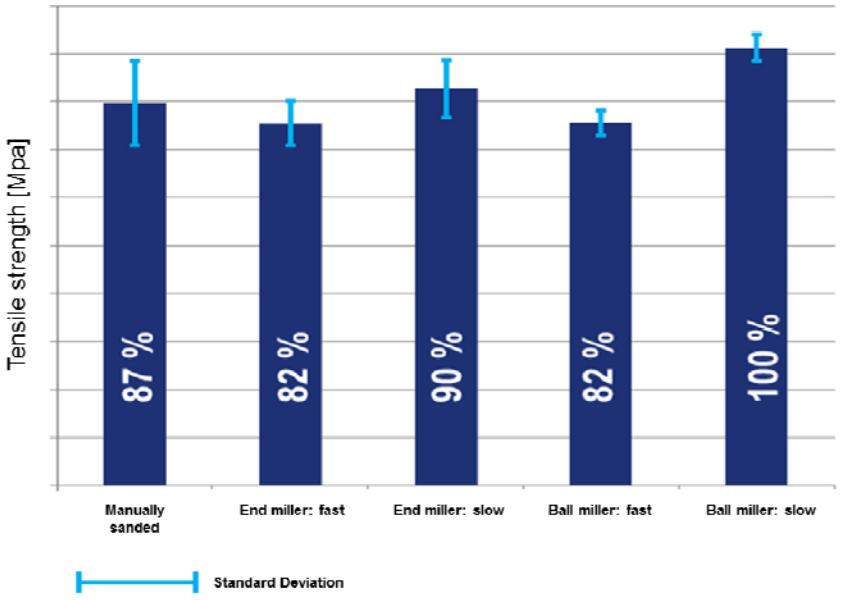

Figure 2-13: Tensile strength results of spliced tensile specimen 1:10.

The evaluation of the sample series with regard to the achieved shear strengths can be seen in Figure 2-14. On the left side of Figure 2-14 every specimen is taken into account, on the right side only the ones with a correct failure mode are considered. Since no single specimen of the parameter set “ball miller fast” showed a correct failure mode, no shear strength value can be calculated (marked red and set to 0% for the diagram with the correct failure modes). As mentioned above, only one specimen showed a correct failure mode for the parameter set “end miller slow”, that’s why no scatter is shown in Figure 2-14 for these specimens.

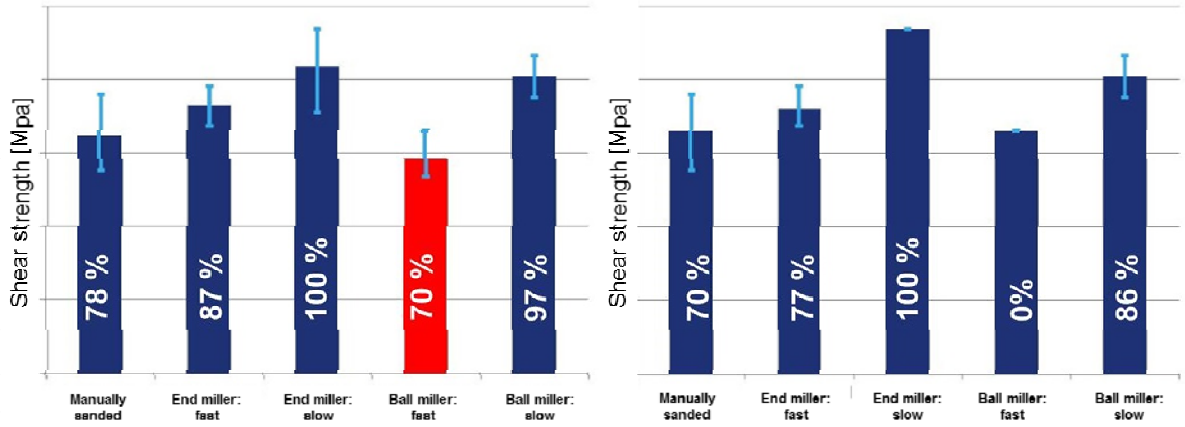

Figure 2-14: Shear strength results of spliced tensile specimen 1:10.

The machining parameters "end miller slow" and "ball miller slow" were chosen as "best" parameter sets due to their failure type. However, the distinction between the other values was difficult because, given a splicing ratio of 1:10 and a sample thickness of 1 mm, only a very small bonding surface is available. This leads inevitably to the fact that already small measurement errors during the determination of the bonding surface lead to large deviations in the absolute values of the shear strength. As expected, the strength results of the 1:60 spliced tensile specimens could not show any differences between the tested parameters, which is why they are not presented separately. This result suggests that a difference in the strength of both methods can not be determined when using a splicing ratio of 1:60 (standard for rotor blade repair).

2.3.3 Summary of the milling parameter analysis

- "End millers" + "Ball miller slow" parameter sets show a homogeneous roughness profile along and transversely to the machining direction.
- Surface differences between the milling parameters + manual processing visible / noticeable
- Surface morphology is the same for both splicing ratios (1:10 and 1:60)
- Alicona roughness measurement shows the same tendencies as tactile roughness measurements however there are different maximum values

Results: Tensile tests 1:10

- The majority of the samples fail in the area of the splicing
- Highest scatter in manual splicing values
- Shear strength values could be faulty → Very small bonding surface → Small inaccuracies have great influence → Maybe better results can be achieved by the use of thicker specimen.

Until now, the mechanical values could not be assigned directly to a determined surface characteristic. The mechanical values determined nevertheless show the parameter set "End miller cutter slow" as the most suitable parameter set for milling of repair splices! It has low scatter, is economical and provides the best combination of mechanical characteristics. (Best shear strength, very good peel and tensile strength)

2.4 Investigation of infusion parameters

On the basis of the results of the RAPID REPAIR project, the manufacturing processes in preform infusion technology were developed further in the CAIRE project. For this purpose, preforming in binder technology

was considered and a screening of existing binder systems as well as activation methods was carried out. In parallel, the process parameters for the manufacturing of a laminate with the required properties were determined.

2.4.1 Determination of infusion temperature

In the first step for finding the optimum process temperature, infusion tests of plates were carried out. The temperature range was derived and defined on the basis of viscosity analysis and preliminary tests. The porosity problem which was detected at temperatures above 100 °C has shown that the process window has to be an ideal compromise between pot life and viscosity. The results of these investigations clearly showed that the process is much more stable and faster at an oven temperature of 60 °C than at 40 °C. The shortest infiltration time was reached at 200 mbar. Here the ratio between permeability of the preform and pressure differential is the most promising. On the basis of these tests and the curing parameters of the resin system used, the oven temperature was set to 65 °C for this resin system.

2.4.2 Determination of infusion pressure

To determine the optimal infusion pressure, the laminate properties of the prepared sample plates were examined with regard to their fiber volume content and their porosity. The target value was a fiber volume content slightly below 50%, as well as a porosity of less than 3%. These values are particularly favorable for the durability of the rotor blade skin and thus for the service life of the repair.

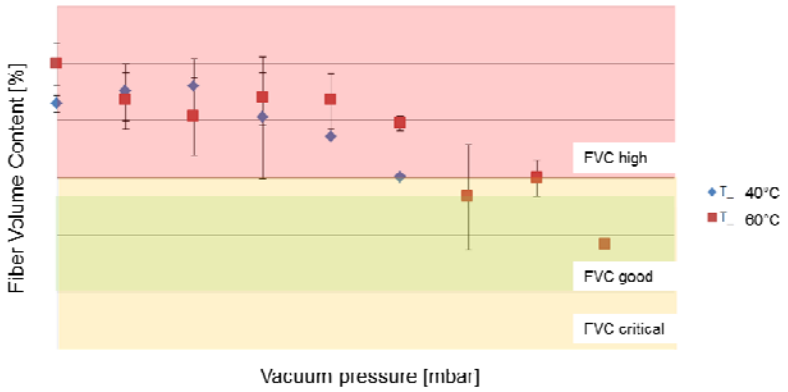

Figure 2-15: Fiber volume content over vacuum pressure.

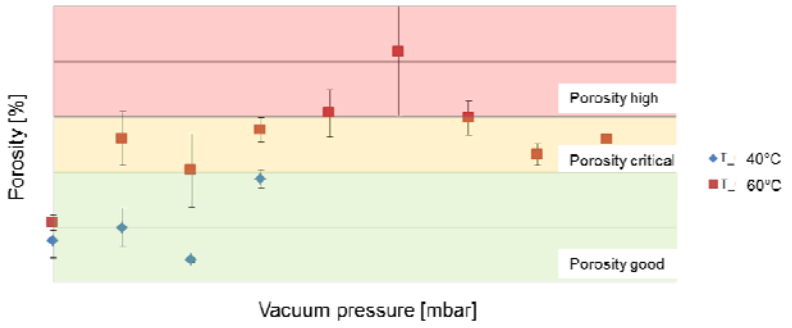

Figure 2-16: Porosity content over vacuum pressure.

Figure 2-15 shows the fiber volume content over the infusion pressure, while Figure 2-16 shows the porosity. The fiber volume content was determined by means of the laminate mass and / or by ashing and later confirmed by a micrograph picture. The porosity was determined by the optical evaluation of the micrographs. In the analysis of the diagrams, it was noticeable that a relatively high infusion pressure is necessary to reach the acceptable fiber volume content below 50%. The porosity of the samples showed exactly the opposite. An acceptable porosity content below 3% could only be achieved at a very low infusion pressure. Due to this contrary behaviour of fiber volume content and porosity it was not possible to find any process parameters that would meet the requirements and target values in the first iteration step. In order to improve the results, a further process variant was used to examine how the good properties of the high and low infusion pressures can be combined. Since the lowest porosity in the previous experiments could be achieved at 0 mbar, full vacuum pressure was also established for the infusion pressure of these tests, but the process was extended by another pressure step with a significantly reduced pressure. By these final additional measures the optimal process parameters could be determined. The following micrographs clearly show the effects of the process parameters on the resulting laminate:

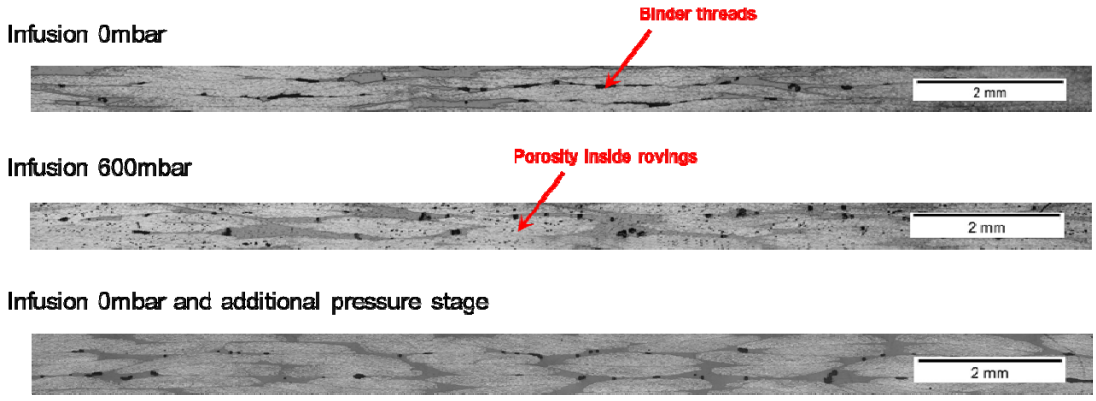

Figure 2-17: Micrographs of infusion laminates manufactured at different vacuum pressures.

The first micrograph in Figure 2-17 shows an infusion followed by curing at maximum vacuum pressure. It is obvious that the rovings are very strongly compressed by the low infusion pressure, resulting in a higher fiber volume content. In addition, the binder threads are visible in the matrix of the laminate. If the micrograph is strongly enlarged, these can be clearly identified and distinguished from porosities. The following section shows an infusion followed by curing at low vacuum pressure. Compared to the previous micrograph, clear porosities are visible even within the rovings. The decreased fiber volume content of this sample can also be recognized by the lower degree of compressing of the rovings in the micrograph. In the lowest section in Figure 2-17, an infusion with the adapted process using an additional pressure stage is shown. It has hardly any porosities and has the desired fiber content of <50%. The method has meanwhile been patented under US2015 / 0145157A1 and EP2875936.

3.0 PREPARING OF CERTIFICATION

As part of the preparation for a possible certification of the procedure, the influence of the binder on the strength of skin repairs had to be investigated. In addition to this, a high number of different coupon and several component test specimens had to be manufactured and tested. The component test specimens should allow the direct comparison between infusion repair with binder preform and hand laminate. For this purpose, two precisely equal-sized repairs with a standard splicing ratio and a characteristic form of a rotor blade skin repair were defined and implemented in one component specimen. A drawing of the repairs is shown in Figure 3-1.

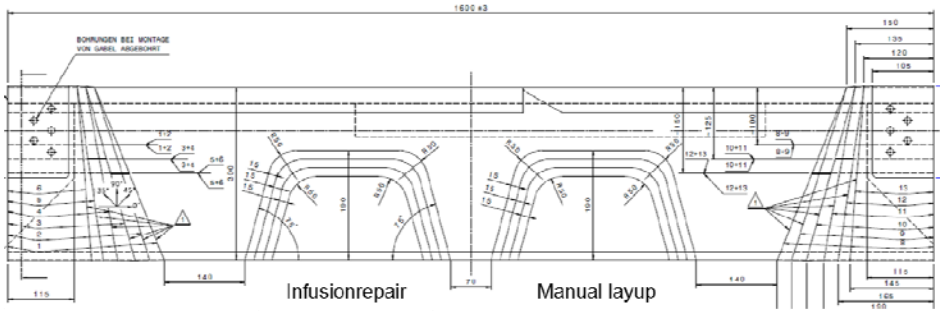

Figure 3-1: Component test specimen for infusion repair.

The splicing of the repairs was carried out manually according to the current state of the art. The "manual repair" was then performed completely according to the current repair instruction. In case of the infusion repair, a dry preform (directly fixed to the peelply via binder) was impregnated via resin infusion from the trailing edge to the leading edge side of the repair. The spliced repair area and the vacuum setup for the infusion repair can be seen on the component test blade in Figure 3-2.

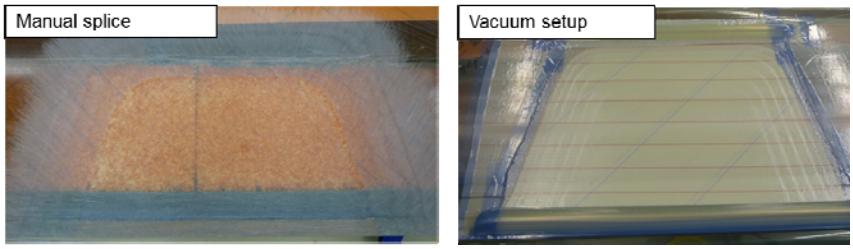

Figure 3-2: Infusion setup for component test specimen.

The infusion of the repair patch worked out as planned. The progress of the infusion as well as the final impregnated repair patch are shown in Figure 3-3.

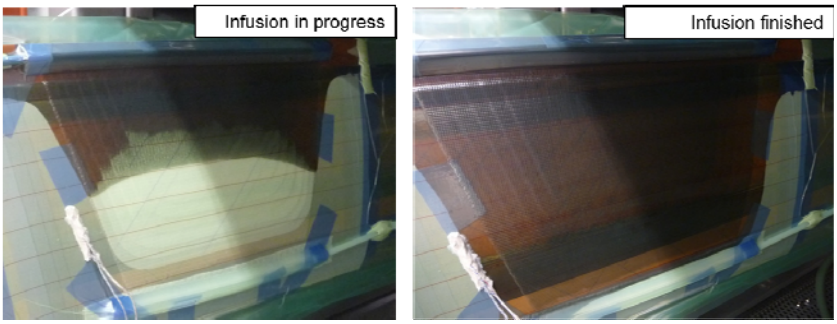

Figure 3-3: Infusion process of component test specimen.

So far, all component test specimens did not show any differences in the strength of the two repairs. In order to manufacture the coupon tests with exactly the same process, the spliced coupons were manufactured with the determined infusion parameters as well. This procedure is shown in Figure 3-4.

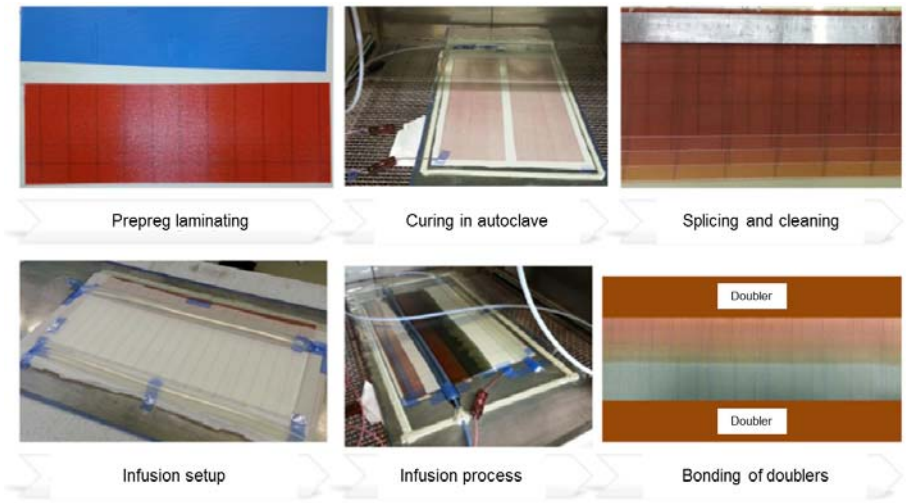

Figure 3-4: Manufacturing of spliced tensile specimen.

The last component tests for the certification of the infusion repair are currently running at Airbus Helicopters in Donauwörth.

4.0 FUTURE PROSPECTS

Due to the automated splicing process and partial automation of the bonding, basic elements have already been developed for the certification of an adhesive bonding process for structural repairs. However, there are still open questions, especially regarding the contamination of bonding surfaces. For these reasons, the certification criteria of EASA (AC 20-107B) currently offer the following options for the approval of structural bonds:

1) Repeatable and reliable non-destructive inspection techniques must be established that ensure the strength of each joint.

→ Technology not available.

2) Full single part testing of bonded joints.

→ Effort not practical

3) Disbonds of each bonded joint greater than the maximum critical disbonding must be prevented by design features.

→ Crack stopper concepts (e.g. rivets)

Since either no technology is available for the first criteria or the implementation is not practicable (second criteria), the only criterion that is used and achievable is number 3. This is not very useful from aerodynamic point of view and not reasonable for bonded joints as well. For this reason, Airbus Helicopters is also participating in the project FACTOR to develop a new approval criterion based on a verifiable and secure bonding process. This process has great potential because it could be used not only for repairs, but also to significantly reduce the weight of the current aircraft by eliminating additional rivets.